Journal of Structural Geology 31 (2009) 842–852

Contents lists available at ScienceDirect

Journal of Structural Geology

journal homepage: www.elsevier.com/locate/jsg

An approach to folding kinematics from the analysis of folded oblique surfaces☆

N.C. Bobillo-Ares [a], F. Bastida [b], J. Aller [b,*], R.J. Lisle [c]

[a] Departamento de Matemáticas, Universidad de Oviedo, 33007 Oviedo, Spain
[b] Departamento de Geología, Universidad de Oviedo, Jesús Arias de Velasco s/n, 33005 Oviedo, Spain
[c] School of Earth and Ocean Sciences, Cardiff University, Cardiff CF10 3YE, UK

ARTICLE INFO

Article history:
Received 6 June 2008
Received in revised form
19 March 2009
Accepted 10 June 2009
Available online 18 June 2009

Keywords:
Folding kinematics
Oblique surfaces
Strain
Computer modelling

ABSTRACT

Two-dimensional analysis of folded surfaces oblique to the mechanical layering can shed light on the kinematic mechanisms that operated during the development of folds. A new version of the program 'FoldModeler', developed in the MATHEMATICA™ environment, is used to obtain the deformed configuration of an initial pattern of oblique surfaces deformed by any combination of the most common kinematic folding mechanisms: flexural flow, tangential longitudinal strain, with or without area change and heterogeneous simple shear. The layer can also undergo any form of homogeneous strain at any moment of the folding process. The outputs of the program provide complete information about the strain distribution in the folded layer that includes graphs of the angle between the oblique surfaces as a function of the inclination of the layering through the fold. These graphs can be very useful to discriminate between the mechanisms that operate in the development of natural folds, and they have been obtained and discussed for the most common combinations of strain patterns. The program is applied to obtain theoretical folds that give a good fit of some natural examples of folded oblique surfaces.

1. Introduction

Folds are structures consisting of a curvature of a set of geological surfaces. In some instances we observe two sets of mutually oblique surfaces affected by folding. Examples of this are found in folded angular unconformities, in folded strata showing cross bedding and in cases where bedding is obliquely cut by sets of cleavage surfaces formed in an earlier folding event. Commonly, the angle between the two sets (obliquity angle) was approximately constant before folding over a distance greater than fold size, but geological experience shows that after folding this angle changes by varying amounts due to the heterogeneous strain associated with folding. The measurements of the obliquity angle in a fold can be plotted graphically as a function of the bedding inclination. The form of this function obviously depends on the folding strain pattern, i.e., on the kinematic folding mechanism.

The analysis of folding of oblique surfaces in rocks serves two main purposes: a) to contribute to the knowledge of strain patterns in folded layers; and b) to decipher the orientation of the oblique surfaces in the configuration prior to folding. The former aim can be achieved in cylindrical folds by analysis of the two-dimensional strain on the profile of the folded layers; however, the achievement of the latter aim requires a three-dimensional analysis of the strain, so that the obliquity angles must be considered as dihedral angles.

The study of folded oblique surfaces has received little attention, and only a few papers have considered this subject (Ramsay, 1961, 1963, 1967, pp. 491–417; Whitten, 1966, pp. 522–532; Coward, 1973; Williams, 1979; Ramsay and Huber, 1987, pp. 476–477 and 484–489; Ramsay and Lisle, 2000, pp. 968–972). Ramsay (1961, 1967) obtained curves of the obliquity angle versus inclination for folds formed by several mechanisms (flexural slip – or flexural flow, flattening and heterogeneous simple shear through the layers). Ramsay and Lisle (2000) made a computer program (DIHEDANGLE.BAS) that gives the modification of the dihedral angle between two planar features as a result of a heterogeneous strain field. With this program the above authors modelled the variation of the dihedral angle as a result of folding by heterogeneous simple shear or heterogeneous simple shear plus flattening.

The present paper is concerned with the application of the analysis of oblique surfaces to the study of folding kinematics. We develop a generalised two-dimensional method to obtain theoretical curves that show the variation of the obliquity angle against bedding inclination for a general folding process in which several buckling mechanisms and other types of strain can be involved. The

☆ The program code ("FoldModelerObliSurf") can be found in the following web page: http://www.geol.uniovi.es/Investigacion/OFAG/Foldteam.html.

* Corresponding author. Tel.: +34 98 510 3119; fax: +34 98 510 3103.
E-mail address: aller@geol.uniovi.es (J. Aller).

0191-8141/$ – see front matter © 2009 Elsevier Ltd. All rights reserved.
doi:10.1016/j.jsg.2009.06.006

theoretical analysis is incorporated in a new version of the program 'FoldModeler' (Bobillo-Ares et al., 2004), which allows the modelling of folds by any simultaneous or successive superposition of flexural flow, tangential longitudinal strain with or without area change, heterogeneous simple shear parallel to the axial trace and any type of homogeneous strain. The program allows the pattern of obliquity angle variation to be determined for folds with different layer geometries (from similar to class 1A; Ramsay, 1967, pp 365–367), surface geometries (from chevron to circular), attitudes (from upright to recumbent) and asymmetries. 'FoldModeler' also calculates a parameter (k) that gives a measure of the quality of the fit between the theoretical curves obtained by the program and the natural data. The parameter k is the root mean square error (RMSE) obtained from the vertical distances between the points corresponding to measurements on the natural fold and the theoretical curve (the coefficient increases with the misfit). Natural points out of the interval of definition of the theoretical curve are not considered in the calculation of k.

After the development of the theoretical basis, patterns of obliquity angle variation versus inclination are characterised for several kinematic folding mechanisms (forward problem). Finally, a few natural examples of folded oblique surfaces are analysed. By comparison of these with theoretically modelled folds conclusions about their folding kinematics are drawn (inverse problem).

2. Modelling folded oblique surfaces

To model folding by different kinematic mechanisms the program 'FoldModeler', developed in the MATHEMATICA™ environment, starts from the initial configuration of a layer profile formed by a grid of squares or rectangles. The nodes of the grid are then displaced according to the transformation relations of the mechanisms involved in folding, and the layer shape and strain state are obtained. In the modelling, it is necessary to initially define the "guideline", a longitudinal reference line located inside the layer that enables the monitoring of folding. In our models, this line has been initially placed in the middle of the layer. The shape of the guideline is defined by a single mathematical function for the two limbs, and the functions used in this paper are conic sections (Aller et al., 2004). The part of a conic section used to represent the fold guideline is defined by its eccentricity e ($0 \leq e < 1$, ellipse; $e = 1$, parabola; $e > 1$, hyperbola), and the aspect ratio h of the fold for symmetrical folds (h is the ratio between the height y_f and the width x_f of a fold limb). In asymmetric folds, the aspect ratio considered is defined for the right limb. The left limb aspect ratio is automatically obtained by the program from the conic eccentricity and the length of the limb. Modelling of folds is achieved by successive or simultaneous superposition of folding steps. Each folding step is defined by the mechanism applied, the increment that it produces in terms of the aspect ratio h of the right limb, and the change that it produces in the eccentricity of the guideline, or by the deformation gradient matrix in the case of a homogeneous strain step. Simultaneous superposition of several mechanisms can be modelled by applying many times in a single run of the program a sequence of folding steps of the involved mechanisms with very small increments in the aspect ratio and shape of the guideline or in the matrix elements that define the homogeneous strain.

To model folding of oblique surfaces, a set of traces with specific inclination is drawn on the initial grid. Each trace is divided into several segments by the intersection points with the lines of the grid, and the position of these points in the initial configuration is calculated by 'FoldModeler'. Once the deformed configuration of the initial squares is obtained applying the transformation relations of the involved mechanisms, the images of the intersection points on the sides of each deformed quadrilateral are determined by maintaining the proportionality relationships of the segments defined by these points on the corresponding side. Joining the images of the different segments of a trace, we obtain the image of the oblique trace. Since the strain is heterogeneous, the accuracy of this method obviously increases as the size of the squares of the grid decreases. Finally, the obliquity angle δ is determined and its variation as a function of the layer inclination α is graphically represented. The way to measure these angles and the sign convention for them is shown in Fig. 1.

3. Folding of oblique surfaces by different folding kinematic mechanisms

To facilitate the analysis of folding of oblique surfaces, curves of the variation with inclination (α) of the obliquity angle (δ) have been generated with 'FoldModeler' for different kinematic mechanisms or superposition of them. In general, for a specific mechanism, the geometry of the curves depends on the geometry of the folded surfaces, the initial ratio between the thickness and length of the layer, the initial dip (δ_0) of the oblique surfaces, assumed constant, and the aspect ratio (h) of the fold. If the oblique surfaces have been generated by the superposition of several mechanisms, the geometry of the curve also depends on the relative amount of each mechanism. There are countless possibilities to model folded oblique surfaces, and in the following text we only show δ–α curves representative of the main kinematic folding mechanisms. These curves allow the main properties of the folding of oblique surfaces for these mechanisms to be inferred (forward problem) and can be also used for obtaining a first indication of the mechanisms that have operated in the development of a specific natural fold with oblique surfaces, whose δ–α curve has been obtained from measurements in the field or photographs (reverse problem). A refinement of the analysis must be made using 'FoldModeler', as it will be described below. The theoretically modelled folds consist of a half wavelength and the thickness/length ratio of the initial layer has been set as 1/30. With exception of the folds formed by pure flexural flow, the geometry of the folded surfaces is parabolic. Likewise, with exception of the folds formed by pure flexural flow and by heterogeneous simple shear, the initial obliquity angle (δ_0) has been set to 30°. One characteristic is that oblique surfaces with opposite signs of the initial obliquity angle (δ_0 and $-\delta_0$) have different curves, although closely related. So if a point (α, δ) belongs to a curve with initial dip δ_0, the point ($-\alpha$, $180 - \delta$) belongs to the curve with initial dip $-\delta_0$ and vice versa. The dominant curvatures of the two curves generally have opposite sign.

3.1. Flexural flow

In this mechanism the strain at a point on the folding layer depends essentially on the inclination at this point with respect to

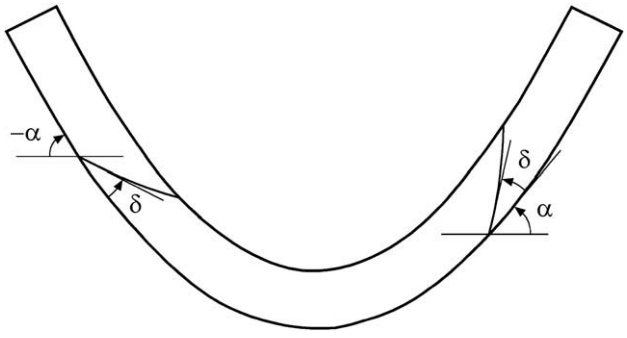

Fig. 1. Sign convention for the obliquity angle δ and the inclination α.

a fixed point without strain (pin point) that is taken as the point whose inclination is zero. This point is generally chosen to be at the hinge point of the folded layer. The strain is independent of the curvature, thickness/length ratio of the layer and fold aspect ratio. Consequently, the δ–α curves are the same for the bottom and the top of the folded layer. A complete analysis of the variation of the dihedral angle between two surfaces for folding by this mechanism was made by Ramsay (1967, pp. 492–498 and Fig. 9–18). Here we present an alternative approach to this problem using 'FoldModeler'. A layer with a set of oblique surfaces folded by this mechanism is shown in Fig. 2a. In this case the guideline is a semi-ellipse that provides an inclination range from -90° to 90° in the construction of the δ–α curves. A complete set of curves of oblique surfaces for intervals of 10° of initial obliquity angle (δ_0) folded by flexural flow are shown in Fig. 3. From this figure we can draw the following conclusions:

- The curves describe decreasing functions.
- Since there is no strain in the hinge point, the initial obliquity angle δ_0 is not modified in this point and the ordinate at the origin of each curve allows the δ_0 value to be inferred.

3.2. Tangential longitudinal strain

Tangential longitudinal strain involves the existence of a neutral surface whose points have no finite strain (neutral points). A layer with a set of oblique surfaces folded by this mechanism is shown in Fig. 2b. Two types of tangential longitudinal strain have been distinguished: parallel and equiareal tangential longitudinal strain (Bobillo-Ares et al., 2006). The former involves area change and constant orthogonal thickness (parallel fold); the latter involves no area change through the fold and produces a thickening of the inner arc part and a thinning of the outer arc part (Ramsay, 1967, pp. 397–403; Bobillo-Ares et al., 2000).

Several pairs of curves, one for the outer arc and other for the inner arc, corresponding to layers folded by parallel tangential longitudinal strain with different aspect ratios h are shown in Fig. 4a. These curves show the following features:

- The δ–α curves are symmetric with respect to the Y-axis.
- The obliquity angle δ increases with respect to δ_0 in the inner arc of the folded layer and decreases in the outer arc. All curves have a turning point at the hinge point; this is a maximum in the inner arc and a minimum on the outer arc.
- The maximum value of the inner arc curves increases as the aspect ratio increases and the outer arc minimum value decreases as this ratio increases.
- Along the neutral line the initial obliquity angle δ_0 does not change with folding. Similarly, this angle barely changes in parts of the layer with high inclinations, where the curvature of the layer is very low. In these zones, the corresponding δ value gives approximately the initial value δ_0.

Folds modelled by tangential longitudinal strain with the same aspect ratio show that the extreme values of δ in the curves deviate from the initial δ_0 value as the layer thickness/length ratio increases; that is, an increase in this ratio has a similar effect that an increase of the aspect ratio.

Representative δ–α curves for folding by equiareal tangential longitudinal strain (Fig. 4b) exhibit similar properties to the

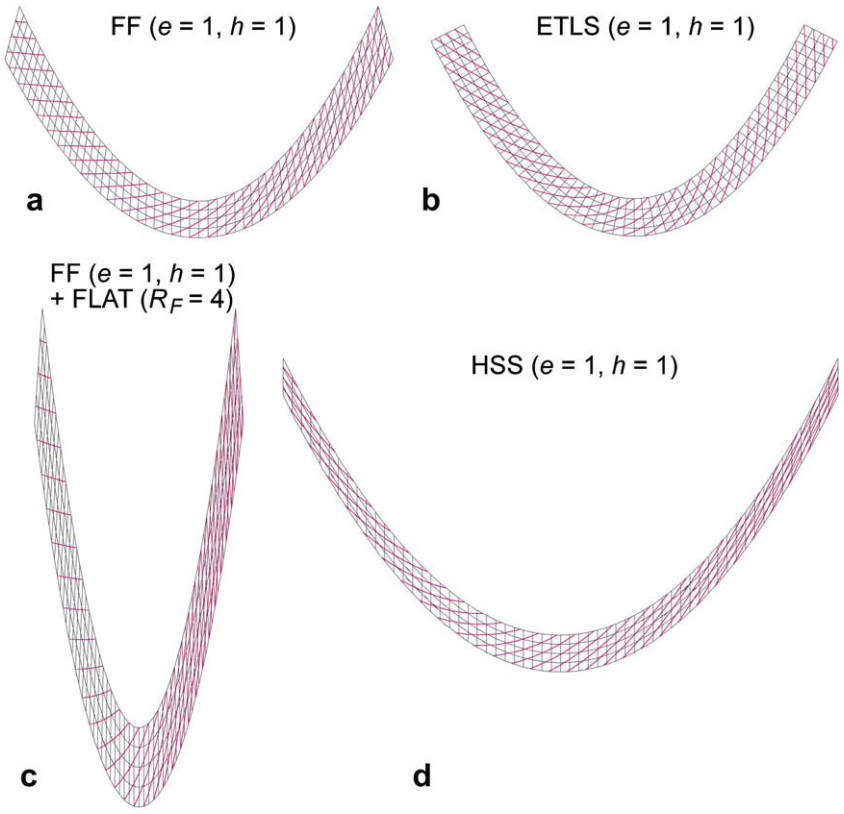

Fig. 2. Folded layers with oblique surfaces obtained with 'FoldModeler' for folding by different kinematic mechanisms. (a) Flexural flow (FF). (b) Equiareal tangential longitudinal strain (ETLS). (c) Flexural flow (FF) plus flattening (FLAT) (R_F is the ratio between major and minor axes of the strain ellipse due to the flattening). (d) Heterogeneous simple shear; the function that describes the displacements of the heterogeneous simple shear is the same that defines the shape of the guideline (parabola, $e = 1$). In all cases the initial obliquity angle is of 30°.

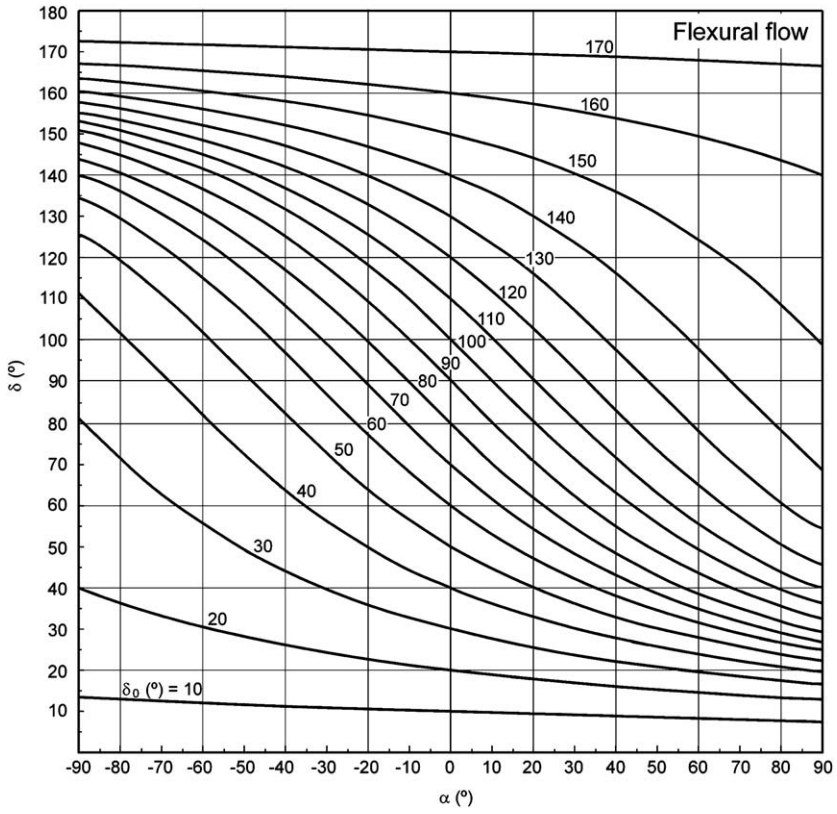

Fig. 3. δ–α curves for folding by flexural flow with several initial obliquity angles (numbers on the curves).

curves of folding by parallel tangential longitudinal strain. The only characteristic difference is that the curves of the inner arc in the equiareal mechanism can be asymmetric, so that the maximum point appears for $\alpha \neq 0$. This asymmetry is more apparent as the fold aspect ratio or the thickness/length of the layer increases, and it is due to the high curvature gradient in the hinge zone that produces an appreciable deviation of the long axes of the strain ellipse from the normal to the layer boundary (Bobillo-Ares et al., 2000).

3.3. Flexural flow or tangential longitudinal strain plus flattening

Flattening of parallel folds has been a mechanism commonly considered to explain the development of class 1C folds or subsimilar folds (Ramsay, 1962, 1967; Mukhopadhyay, 1965; Hudleston, 1973). In this section, flattening of folds previously formed by buckling mechanisms (flexural flow or tangential longitudinal strain) will be considered.

Oblique surfaces folded by flexural flow plus flattening were analysed by Ramsay (1967, pp. 498–500, Fig. 9–19), who showed several representative δ–α curves. A layer with a set of oblique surfaces folded by this combination of mechanisms flexural flow plus flattening is shown in Fig. 2c, and a set of δ–α curves is shown in Fig. 5a. The aspect ratio of the fold by flexural flow is $h = 1$, and the amount of flattening is given on the curves by the value of $R_F = \sqrt{\lambda_1/\lambda_2}$, where λ_1 and λ_2 are the principal quadratic elongations due to the flattening. The curves show that as the flattening amount increases a more definite turning point more appears. This

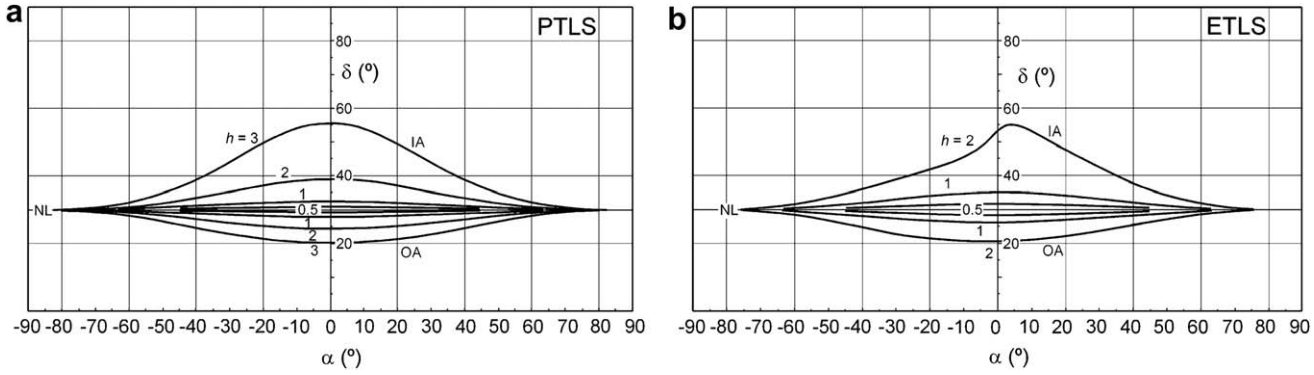

Fig. 4. δ–α curves for folding by parallel (a) and equiareal (b) tangential longitudinal strain with different aspect ratio (numbers on the curves), an initial ratio between the thickness and length of the layer of 1/30 and parabolic neutral line (NL). Curves above the neutral line correspond to the inner arc (IA) and curves below the neutral line correspond to the outer arc (OA). The initial obliquity angle is of 30°.

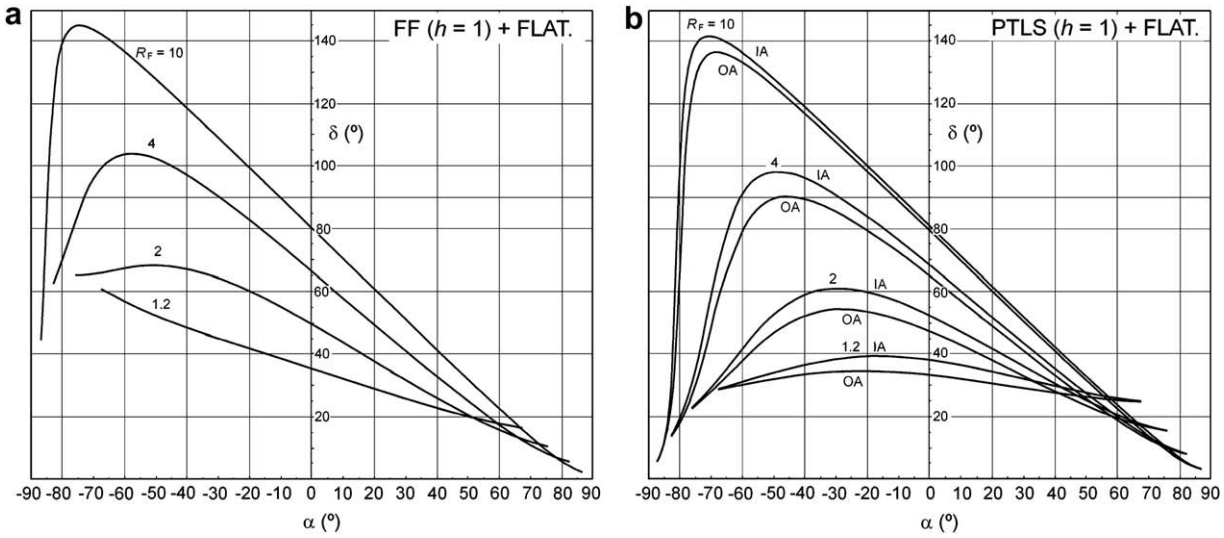

Fig. 5. δ–α curves for folding by flexural flow (FF) plus flattening (FLAT) (a) and by parallel tangential longitudinal strain (PTLS) plus flattening (FLAT) of a layer with an initial ratio between the thickness and length of the layer of 1/30 and parabolic neutral line. (b). Numbers on the curves represent the ratio (R_F) between the major and the minor axes of the strain ellipse due to flattening. In (b), IA = inner arc, and OA = outer arc. The initial obliquity angle is of 30°.

point is located on a limb and migrates with flattening towards points with greater absolute values of inclination.

The curves representative of parallel tangential longitudinal strain, with $h = 1$, plus flattening (Fig. 5b) show that the turning points are displaced progressively towards a limb as the flattening amount increases and the minimum of the outer arc, typical of the tangential longitudinal strain, becomes a maximum. With high flattening the curves can be difficult to distinguish from the curves corresponding to flexural flow plus flattening. The main differences between the two cases are the following (Fig. 5):

- For low amounts of flattening, the maximum is better defined for parallel tangential longitudinal strain plus flattening.
- For high values of flattening the curve is the same for the bottom and the top of the layer in flexural flow plus flattening, but this does not occur for parallel tangential longitudinal strain, with $h = 1$, plus flattening. However, in cases in which the δ_0 value is different for the top and the bottom of the layer, or this angle is only measurable in a boundary of the layer, this difference is not applicable to natural folds.
- The decreasing part of the curves located on the left of the maximum point in Fig. 5 is more developed in the folds formed by parallel tangential longitudinal strain plus flattening than in the folds formed by flexural flow plus flattening.

The δ–α curves for folding by equiareal tangential longitudinal strain plus flattening can be very difficult to distinguish from those of folding by parallel tangential longitudinal strain plus flattening. Nevertheless, when the initial thickness/length ratio of the layer is high and the equiareal tangential longitudinal strain produces a bulge in the inner arc with a multiple hinge, the flattening amplifies the bulge and the δ–α curve has a characteristic anomaly and is a multiform function in the interval with low inclinations (several δ values for each single α value). These are diagnostic features of equiareal tangential longitudinal strain.

3.4. Flexural flow or tangential longitudinal strain plus homogeneous simple shear perpendicular to the axial trace

Superposition of homogeneous or near homogeneous simple shear over previous folds has been proposed by several authors to explain the development of overturned or recumbent folds (e.g., Hudleston, 1977; Ramsay et al., 1983; Fernández et al., 2007). Two sets of δ–α curves for folding by flexural flow plus simple shear are shown in Fig. 6 for a $\delta_0 = 30°$. Fig. 6a corresponds to negative simple shear (anticlockwise rotation). In this case, the curves are comparable to those of flexural flow plus flattening or tangential longitudinal strain plus flattening. Fig. 6b corresponds to positive simple shear. In this case the δ–α curves are mainly decreasing, and a maximum point only appears for high values of the shear strain ($\gamma = 3$). This is different to the cases with negative simple shear or flattening.

δ–α curves for folding by parallel tangential longitudinal strain plus simple shear are shown in Fig. 7. In these cases, the differences due to the sign of the simple shear are less than in the cases of flexural flow plus simple shear, because a well defined maximum appears in all cases. However, the position of this maximum point allows the sign of the simple shear to be discriminated in the cases with low values of the shear strain. In the cases with high values of the shear strain the discrimination by the form of the curves is very difficult; nevertheless the sense of the fold asymmetry allows the differentiation to be easily made in any case. A similar problem is posed to distinguish the flexural flow plus flattening from the parallel tangential longitudinal strain (or equiareal tangential longitudinal strain) (compare Fig. 7 with Fig. 6a).

3.5. Heterogeneous simple shear

Whether shear folds – similar folds formed by heterogeneous simple shear parallel to the axial plane – truly exist in nature has been a controversial matter (e.g, González-Bonorino, 1960; Ramberg, 1963; Ramsay, 1967, pp. 421–423; Ragan, 1968, p. 46; Hudleston, 1977), because it involves some conditions that are difficult to justify in natural folds. Among others, it produces strain patterns that do not agree with those usually deduced from the cleavage distribution in similar or subsimilar folds. In addition, when the shear direction is perpendicular to the initial layer, it does not produce shortening in a direction perpendicular to the axial plane. Nevertheless, this mechanism is geometrically possible and a heterogeneous simple shear component could operate in combination with other kinematic mechanisms. In fact, surfaces folded by this mechanism have been analysed by several authors, and the corresponding δ–α curves were shown by Ramsay (1967,

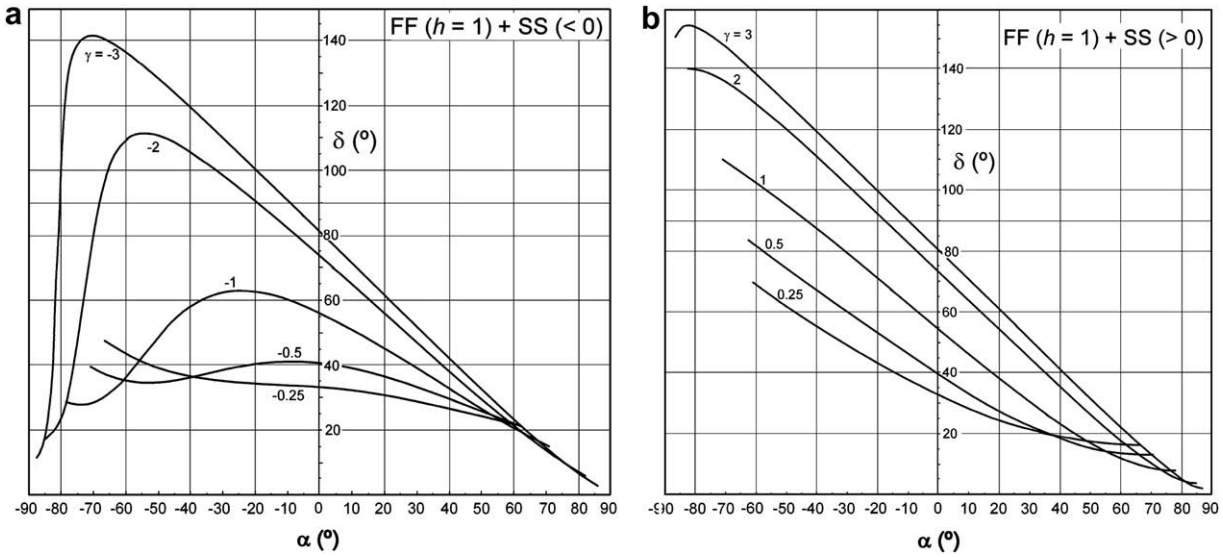

Fig. 6. δ–α curves for folding by flexural flow (FF) and homogeneous simple shear (SS) perpendicular to the axial trace. (a) The rotation sense is anticlockwise (SS < 0). (b) The rotation sense is clockwise (SS > 0). Numbers on the curves represent the shear strain (γ). The initial obliquity angle is of 30°.

Fig. 9–30), Williams (1979, Fig. 5c) and Ramsay and Lisle (2000, Fig. 36–71). Hence, this mechanism has been included in the program 'FoldModeler' and considered in the analysis of oblique surfaces. In any case, the comparison of the theoretical results produced for this mechanism with the characteristics of natural folds can provide good arguments to know if heterogeneous simple shear is a mechanism that operates in natural folds.

A layer with a set of oblique surfaces folded by heterogeneous simple shear is shown in Fig. 2d. As with the mechanism of flexural flow, in heterogeneous simple shear the obliquity angle δ is independent of the curvature, thickness/length ratio of the layer and fold aspect ratio. Fig. 8a shows a set of δ–α curves of folds modelled by heterogeneous simple shear with different values of the initial obliquity angle δ_0. Except the curve with $\delta_0 = 90°$, which corresponds to the straight line $\delta = 90 - \alpha$, the curves have a turning point (maximum when $\delta_0 < 90°$ and minimum when $\delta_0 > 90°$), whose corresponding inclination value depends on the δ_0 value. These curves are difficult to distinguish from those obtained for flexural flow or tangential longitudinal strain plus flattening. A peculiar characteristic of these curves is that they pass through the points (−90, 0) and (90, 0). This can be a distinctive feature, but only when high inclinations appear in the fold. As in flexural flow, when the initial obliquity angle δ_0 has the same value for the top and the bottom of the layer, the curve is the same for the two layer boundaries; this feature can help to distinguish heterogeneous simple shear from other mechanisms.

3.6. Heterogeneous simple shear parallel to the axial plane plus flattening

This mechanism has been proposed by several authors (Ramsay, 1967, pp. 421–436; Hudleston, 1977; Ramsay and Lisle, 2000, p. 824

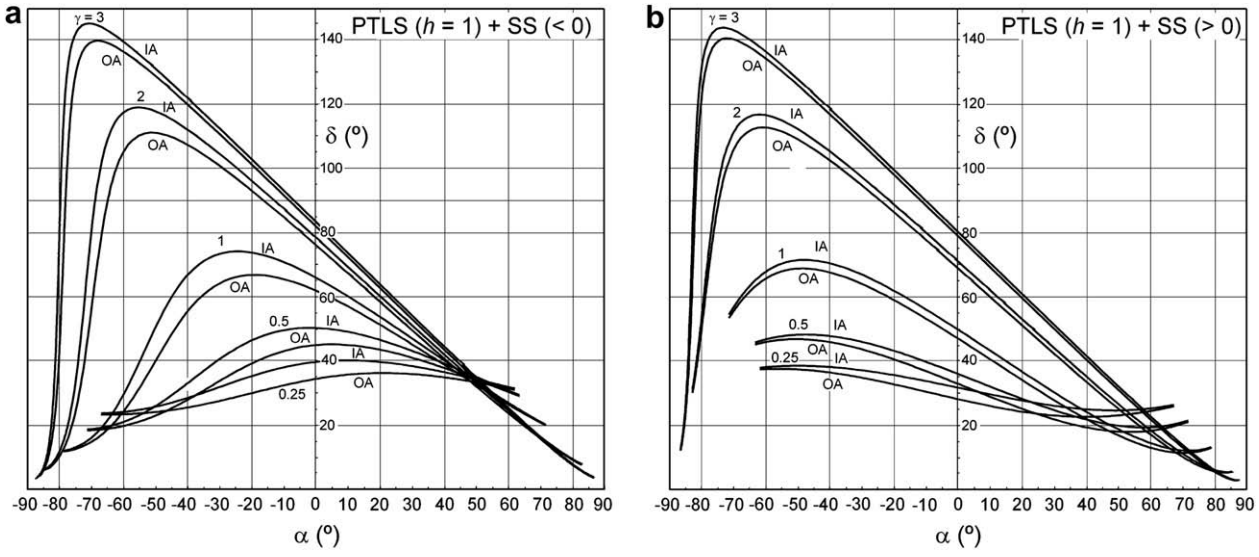

Fig. 7. δ–α curves for folding by parallel tangential longitudinal strain (PTLS) and homogeneous simple shear (SS) perpendicular to the axial trace of a layer with an initial ratio between the thickness and length of the layer of 1/30 and parabolic neutral line. (a) The sense of the displacements is the same of the initial dip direction of the oblique surfaces (SS < 0). (b) The sense of the displacements is opposite to the dip direction of the oblique surfaces (SS > 0). Numbers on the curves represent the shear strain (γ). The initial obliquity angle is of 30°.

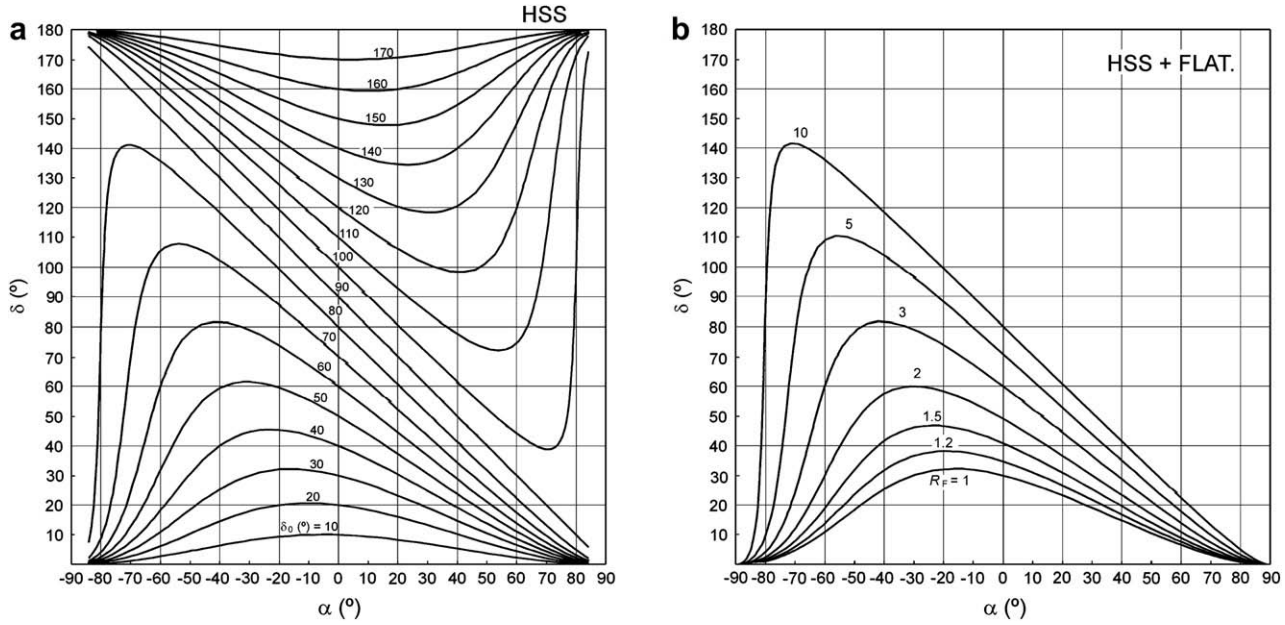

Fig. 8. (a) δ–α curves for folding by heterogeneous simple shear (HSS) with several initial obliquity angles (numbers on the curves). (b) δ–α curves for folding by heterogeneous simple shear (HSS) plus flattening (FLAT); numbers on the curves represent the ratio (R_F) between the major and the minor axes of the strain ellipse due to flattening; the initial obliquity angle is of 30°.

and 826–831) to explain the development of similar folds. These authors obtained δ–α curves for oblique surfaces folded by this superposition of strain patterns (Ramsay, 1967, Fig. 9–31; and Ramsay and Lisle, 2000, Fig. 36.71). The inclusion of flattening eliminates some of the problems of the heterogeneous simple shear mechanism, since flattening gives rise to shortening perpendicular to the axial plane and produces strain patterns compatible with the cleavage distribution observed in natural folds. An interesting aspect is that, in this type of superposition, the application order of the mechanisms does not influence the form of the δ–α curve although it influences the geometry of the final fold, i.e., the superposition is commutative for the curves but not for the folds (Appendix A). As a consequence of this, the curves corresponding to this combination of mechanisms (Fig. 8b) are indistinguishable from those obtained in a single episode of heterogeneous simple shear, since the δ–α curve of a fold formed by a component of flattening and another of heterogeneous simple shear can be also obtained by heterogeneous simple shear on a layer with a different initial dip δ_0 that incorporates the effect of the flattening component on the initial layer.

4. Application to the analysis of natural folds

When the curves that describe the δ vs. α variation are available for a natural fold, the graphs obtained in the previous section can be used to gain some insight into the folding mechanisms involved in the development of the fold. On the other hand, 'FoldModeler' can be used in this case to find by a trial-and-error method a particular combination of mechanisms that gives the best fit to all the geometrical features of the natural fold. Two natural examples have been selected to explore the potentials of this method. The first of them corresponds to a slightly asymmetric anticline developed in a unit of Cambrian sandstone and shale of the Westasturian-Leonese zone near Cudillero (Asturias, Spain). The sandstone layers A and B pictured in Fig. 9a show a folded pattern of cross bedding that has been sketched in black in Fig. 9b. Points in the graphics of Fig. 9c and d indicate the variation of the obliquity angle δ along the folded layer for the top of layers A and B respectively. Note that as 'FoldModeler' only models synforms and has a particular convention to measure angles (shown in Fig. 9b), the left part of the layer is represented in the right part of the diagram and vice versa. A good fit to the geometrical features of these folds can be been obtained with the following modelling parameters: Layer A: Guideline eccentricity = 0 (circular arc) and a superposition of a first folding increment of tangential longitudinal strain without area change ($\Delta h = 0.28$ measured in the right limb) and a second event of flexural flow ($\Delta h = 0.56$ measured in the right limb). The δ–α curve for this fold is represented in green in Fig. 9c, in which curves for pure tangential longitudinal strain with area change and flexural flow are also displayed to allow comparison. Good fits can be also obtained if the application order of the two mechanisms is reversed, but the relative intensity of the flexural flow episode must be increased. Tangential longitudinal strain preceding flexural flow is suggested by the analysis of other folds in the area (Toimil and Fernández, 2007). Layer B: Guideline eccentricity = 0.6 (ellipse arc) and a single folding episode of flexural flow ($h = 1$ in the right limb). The initial obliquity angle (δ_0) is 160° for the two layers, though a better fit for the leftmost part of layer B (rightmost part of the diagram of Fig. 9d) is obtained with $\delta_0 = 154°$. The 'FoldModeler' output with the deformed grids of quadrilaterals (green) and the deformed traces (red) is shown in Fig. 9b superposed on the sketch of the natural fold.

The analysis of folded oblique surfaces using 'FoldModeler' has been also applied to a minor fold developed in a psammite layer near Rhoscolyn Head (Holy Island, North Wales) during a second deformation event that modified and distorted a previous hectometric anticline and gave rise to minor folds and crenulation cleavage S_2 (Cosgrove, 1980; Lisle, 1988; Treagus et al., 2002). Oblique surfaces analysed in this case are S_1 surfaces folded into a minor D_2 synform. Fig. 10a shows the studied fold with a superposed sketch of bedding (blue lines), folded S_1 surfaces (red lines) and the reference frame used for the measure of angles. Fig. 10b and d allows comparison between the obliquity angles measured on the photograph (points) and those obtained for the theoretical fold shown on Fig. 10c (green lines). The theoretical fold was obtained with 'FoldModeler', applying to a horizontal layer a folding sequence with guideline eccentricity = 1.2 (hyperbola arc) and

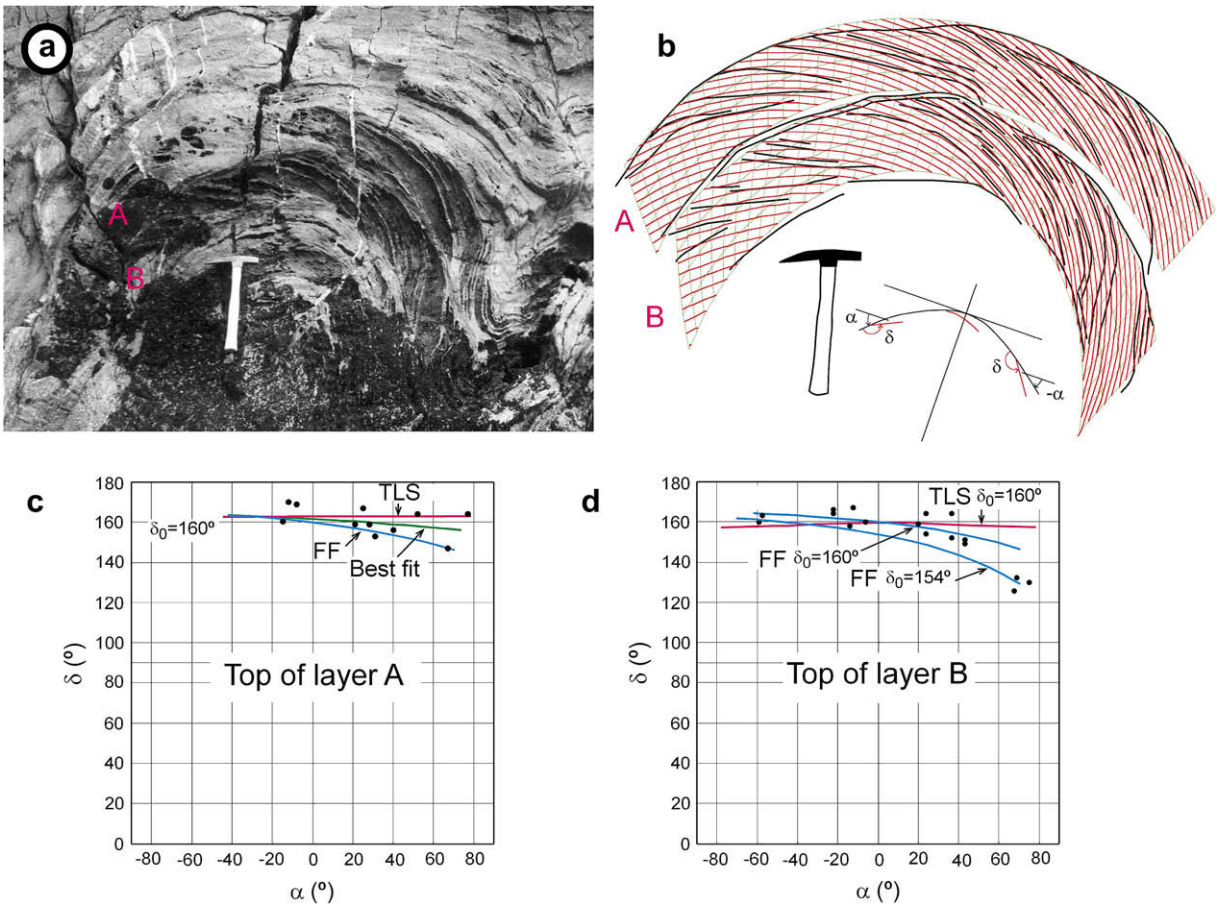

Fig. 9. (a) Anticline developed in Cambrian sandstone and shale of the Westasturian-Leonese zone near Cudillero (Asturias, Spain) showing a folded pattern of cross bedding. (b) Sketch of the natural folded oblique surfaces (in black) with the theoretical fold obtained with 'FoldModeler' superposed (layer boundaries and grid in green and oblique surfaces in red); the sign convention is shown. (c) and (d) Variation of the obliquity angle δ along the folded layer for the top of layers A and B respectively. Points correspond to natural data; the green curve is the best fit obtained for layer A (RMSE parameter $k = 5.9$); red curves correspond to a mechanism of pure tangential longitudinal strain without area change ($k = 7.05$ for layer A and 7.3 for layer B); blue curves correspond to a pure flexural flow mechanism ($k = 6.54$ for layer A and 4.36 for layer B with $\delta_0 = 160°$, the curve corresponding to $\delta_0 = 154°$ has been constructed to fit the points with α between 60 and 80°).

involving three folding steps: i) Tangential longitudinal strain without area change ($\Delta h = 0.2$), ii) Flexural flow ($\Delta h = 0.3$), and iii) Homogeneous flattening perpendicular to the axial plane with $\sqrt{\lambda_1/\lambda_2} = 3.24$. The initial obliquity angle (δ_0) was 30°. Curves corresponding to pure tangential longitudinal strain plus homogeneous flattening and pure flexural flow plus homogeneous flattening are also shown in Fig. 10b and d to allow comparison. The different attitude of the natural and the theoretical fold (Fig. 10a and c) is probably due to the formation of the former in a second deformation event on a layer dipping as a result of the first deformation, whereas the theoretical fold was modelled from a horizontal layer. The fit obtained suggests that the deformation sequence of the theoretical fold can be considered as a first approach to the one which operated in the natural fold, though some mechanisms that cannot be introduced in the 'FoldModeler' analysis cannot be discarded. This is the case of a possible role of active folding during the last stage that gave rise to the synform drawn by S_1 in the left limb of the fold analysed. The thinning of the layer towards the left can be interpreted as a feature previous to folding that can be tentatively attributed to pinch and swell structures developed in the limb of a D_1 fold due to flattening associated with this deformation phase. 'FoldModeler' cannot produce folds from a layer with variable thickness and hence the precise form of the folded layer could not be reproduced in the model. Theoretical folds that reproduce the thinning observed in the psammite layer and give a reasonably good fit to the δ variation throughout the fold can be obtained applying simple shear deformation to the model, but they do not agree with the deformation sequence of the area nor with the geometries of other folds observed in the outcrop (Lisle, 1988; Treagus et al., 2002).

5. Conclusions

Analysis of folded oblique surfaces can provide an interesting contribution to the discrimination of kinematic mechanisms that operated during folding. The program 'FoldModeler' allows modelling oblique surfaces folded by any successive or simultaneous superposition of the main kinematic folding mechanisms and facilitates a general method to make this analysis on the fold profiles. The graphical representation of the obliquity angle δ as a function of the inclination α (δ–α curve) is the tool used to carry out the discrimination. 'FoldModeler' allows obtaining a lot of δ–α curves in a short interval of time.

The discrimination between the two basic mechanisms of buckling (flexural flow and tangential longitudinal) is simple when superposed homogeneous strain did not operate. The δ–α curves of folds formed by flexural flow are monotonously decreasing and, when the initial obliquity angle δ_0 is the same for the top and bottom of the layer, the δ–α curve is also the same for the two layer boundaries. On the other hand, the δ–α curves of folds formed by

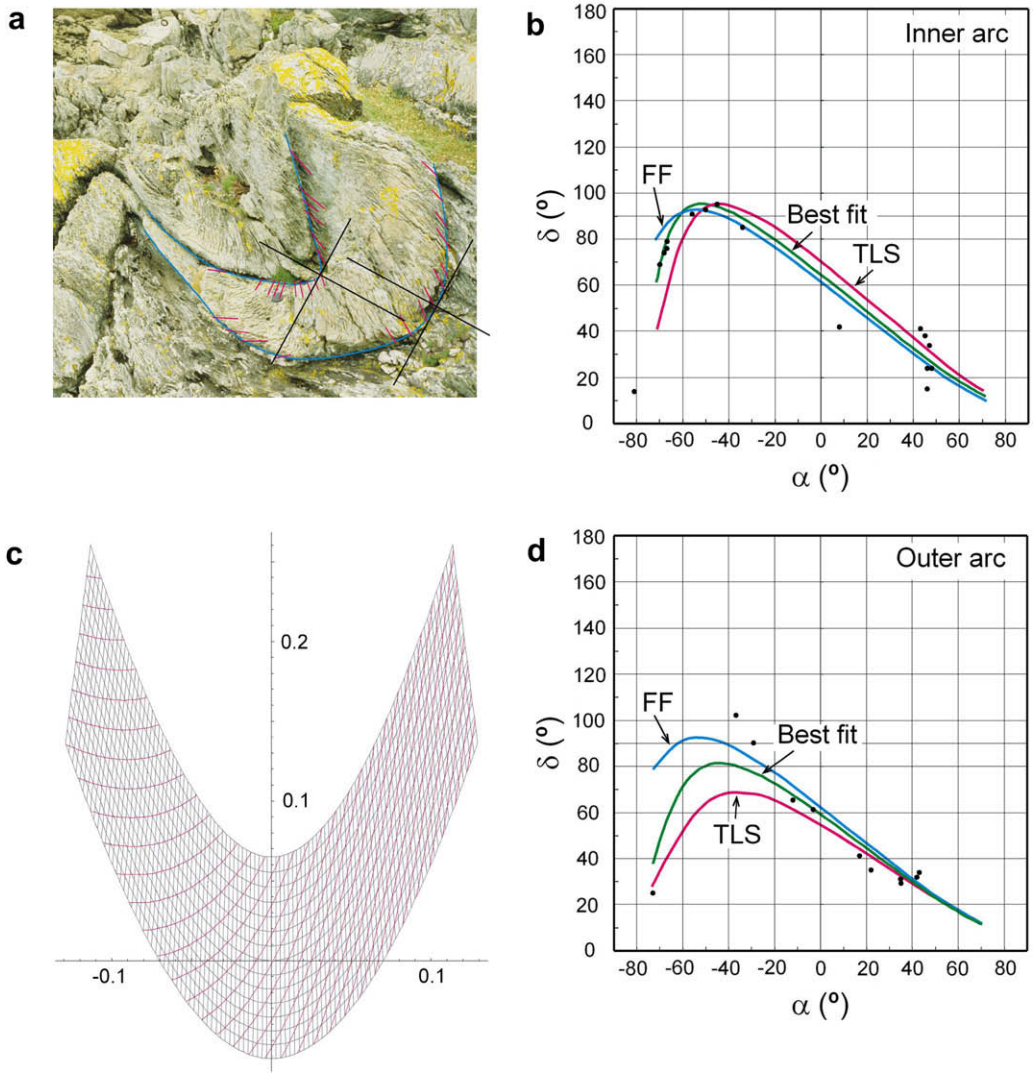

Fig. 10. (a) Minor fold developed in a psammite layer near Rhoscolyn Head (Holy Island, North Wales) with a superposed sketch of bedding (blue lines), folded S_1 surfaces (red lines) and the reference frame used for the measure of angles. (b) and (d) Variation of the obliquity angle δ along the folded layer for the inner arc and the outer arc respectively; points correspond to natural data; green curves correspond to the theoretical best fit obtained ($k = 7.33$ for the inner arc and 9.54 for the outer arc); blue curves correspond to pure flexural flow plus flattening ($k = 9.12$ for the inner arc and 18.79 for the outer arc); red curves correspond to the pure tangential longitudinal strain without area change plus flattening ($k = 13.57$ for the inner arc and 12.67 for the outer arc). (c) Theoretical fold obtained with 'FoldModeler' to fit the natural fold.

tangential longitudinal strain are in general symmetrical with a turning point at the hinge point ($\alpha = 0$). These curves are different for the two layer boundaries and the turning point is a maximum in the inner arc and a minimum on the outer arc. An exception appears for equiareal tangential longitudinal strain, in which the maximum of the curve can appear slightly outside the point with $\alpha = 0$ and the curve can be somewhat asymmetric when the thickness/length ratio of the initial layer or the aspect ratio of the fold is high.

The superposition of a flattening or a homogeneous simple shear parallel to the axial trace on folds previously formed by flexural flow or tangential longitudinal strain gives rise to changes in the form of the δ–α curves. If low homogeneous strain is involved in the superposition, these curves can allow the discrimination of the kinematic mechanisms involved in the folding by inspection about the existence of a maximum point and its location when it exists. When high homogeneous strain is superposed on previous folds, a convergence in the form of the curves is produced, so that these present a prominent maximum point in the high inclination part of a limb. In these cases, the discrimination of the kinematic mechanisms involved in the folding is difficult. An exception is the case of flexural flow plus homogeneous simple shear with a shear direction opposite to the initial dip of the oblique surfaces. In this case, a maximum point only appears for very high levels of strain and near to an end of the curve.

The δ–α curves corresponding to folds formed by heterogeneous simple shear are comparable to those for folds modified by flattening or homogeneous simple shear, although the initial obliquity angles are very different for these curves. When shear folds are flattened, their curves are very difficult to distinguish from those corresponding to other types of flattened or sheared folds.

When shear folds are combined with an irrotational homogeneous strain with the maximum elongation direction perpendicular to the original layer, the order of application of the kinematic mechanisms influences the geometry of the folded layer but not the form of the δ–α curve.

The use of standard sets of curves corresponding to different types of strain patterns can be a valuable method to obtain a first indication about the kinematic mechanisms that operated in a specific natural fold, mainly when other geological information about the structure is available. However, the search for a specific

δ–α curve that precisely fits the points (α, δ) measured from the natural fold can provide a more exact determination of the mechanisms involved. This can be made by trial-and-error using the program 'FoldModeler'.

Acknowledgements

The present work was supported by Spanish CGL-2006-06401-BTE project funded by Ministerio de Educación y Ciencia and Fondo Europeo de Desarrollo Regional (FEDER). We are grateful to P.J. Hudleston and R.J. Twiss for many valuable suggestions that notably improved the manuscript.

Appendix A. Commutativity of the superposition of heterogeneous simple shear and flattening for the functional relation between δ and α

Let h be the deformation gradient, $\mathbf{U}$ and $\mathbf{u}$ the vectors indicating the layer inclination before and after folding, and $\mathbf{V}$ and $\mathbf{v}$ the vectors indicating the trace direction of the oblique surface before and after the folding (Fig. A1). We have that

$$\mathbf{u} = h\mathbf{U}, \quad \mathbf{v} = h\mathbf{V} \tag{A1}$$

The angles searched are determined by the following geometrical relationships:

$$\cos\delta = \frac{\mathbf{u}\cdot\mathbf{v}}{|\mathbf{u}||\mathbf{v}|}, \quad \tan\alpha = \frac{\mathbf{u}\cdot\hat{\mathbf{j}}}{\mathbf{u}\cdot\hat{\mathbf{i}}}, \tag{A2}$$

where $\hat{\mathbf{i}}$ and $\hat{\mathbf{j}}$ are the unit vectors of the orthonormal basis $e = (\hat{\mathbf{i}}, \hat{\mathbf{j}})$ (Fig. A1).

Specifically, we will determine these angles in two cases: 1) heterogeneous simple shear plus flattening, and 2) flattening plus heterogeneous simple shear. In the two cases the matrices of the objects will be referred to the basis e. These matrices will be named by a subscript e; for example, h_e and $\mathbf{v}_e$ are the matrices of h and $\mathbf{v}$ in that basis.

Case 1 heterogeneous simple shear plus flattening

The equations of the total transformation are:

$$\left.\begin{aligned} x &= AX \\ y &= Baf(X/a) + BY \end{aligned}\right\}, \tag{A3}$$

where $f(X/a)$ is the equation of the conic that represents the guideline and a the scale factor of this curve. We obtain directly the following matrices:

$$h_e^{(1)} = \begin{pmatrix} A & 0 \\ Bf'(X/a) & B \end{pmatrix}, \quad \mathbf{U}_e = \begin{pmatrix} 1 \\ 0 \end{pmatrix}, \quad \mathbf{V}_e = \begin{pmatrix} \cos\delta_0 \\ \sin\delta_0 \end{pmatrix}, \tag{A4}$$

where $f'(X/a)$ is the derivative of f at the value X/a. Then, the vector $\mathbf{u}_e^{(1)}$ is given by:

$$\mathbf{u}_e^{(1)} = h_e^{(1)}\mathbf{U}_e = \begin{pmatrix} A \\ Bf'(X/a) \end{pmatrix}, \quad \text{and} \quad \tan\alpha^{(1)} = \frac{B}{A}f'(X/a). \tag{A5}$$

With this equation for $\tan\alpha^{(1)}$ we can write $h_e^{(1)}$ and $\mathbf{u}_e^{(1)}$ in the following form:

$$h_e^{(1)} = \begin{pmatrix} A & 0 \\ A\tan\alpha^{(1)} & B \end{pmatrix} \quad \mathbf{u}_e^{(1)} = \begin{pmatrix} A \\ A\tan\alpha^{(1)} \end{pmatrix} \tag{A6}$$

The vector $\mathbf{v}_e^{(1)}$ is calculated using the $h_e^{(1)}$ value given in (A6)and the $\mathbf{V}_e$ value given in (A3), i.e.,

$$\mathbf{v}_e^{(1)} = h_e^{(1)}\mathbf{V}_e = \begin{pmatrix} A\cos\delta_0 \\ A\tan\alpha^{(1)}\cos\delta_0 + B\sin\delta_0 \end{pmatrix} \tag{A7}$$

Case 2 flattening plus heterogeneous simple shear

In this case, the equations of the total transformation are:

$$\left.\begin{aligned} x &= AX \\ y &= Aaf(X/a) + BY \end{aligned}\right\}. \tag{A8}$$

Comparing equations (A8) with those (A3) we observe that both are different and then, the folds formed in the cases 1) and 2) may be different.

The matrix of the deformation gradient is

$$h_e^{(2)} = \begin{pmatrix} A & 0 \\ Af'(X/a) & B \end{pmatrix}, \tag{A9}$$

and therefore,

$$\mathbf{u}_e^{(2)} = h_e^{(2)}\mathbf{U}_e = \begin{pmatrix} A \\ Af'(X/a) \end{pmatrix}, \quad \text{and} \quad \tan\alpha^{(2)} = f'(X/a). \tag{A10}$$

Introducing this value of $\tan\alpha^{(2)}$ in the previous matrix $h_e^{(2)}$, we have:

$$h_e^{(2)} = \begin{pmatrix} A & 0 \\ A\tan\alpha^{(2)} & B \end{pmatrix} \quad \text{and} \quad \mathbf{u}_e^{(2)} = \begin{pmatrix} A \\ A\tan\alpha^{(2)} \end{pmatrix}, \tag{A11}$$

and finally

$$\mathbf{v}_e^{(2)} = h_e^{(2)}\mathbf{V}_e = \begin{pmatrix} A\cos\delta_0 \\ A\tan\alpha^{(2)}\cos\delta_0 + B\sin\delta_0 \end{pmatrix}. \tag{A12}$$

As we can see in (A2), the calculation of δ is made in terms of $\mathbf{u}$ and $\mathbf{v}$. On the other hand, the form of the matrices $\mathbf{u}_e^{(1)}$ and $\mathbf{v}_e^{(1)}$ in terms of $\tan\alpha^{(1)}$ [eq. (A6 and A7)] is the same than those of $\mathbf{u}_e^{(2)}$ and $\mathbf{v}_e^{(2)}$ in terms of $\tan\alpha^{(2)}$ [eq (A11) and (A12)]. Hence, although the folded layers are different in the two cases, the relations between δ and α are identical.

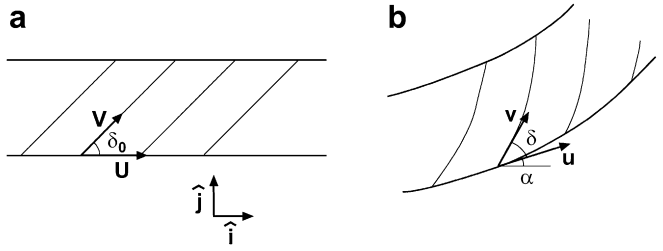

Fig. 1A. Vectors used to define the directions of the layer boundary and the oblique surface in the initial (a) and the final (b) configurations. $\hat{\mathbf{i}}$ and $\hat{\mathbf{j}}$ are the unit vectors of the reference orthonormal basis.

References

Aller, J., Bastida, F., Toimil, N.C., Bobillo-Ares, N.C., 2004. The use of conic sections for the geometrical analysis of folded surface profiles. Tectonophysics 379, 239–254.

Bobillo-Ares, N.C., Aller, J., Bastida, F., Lisle, R.J., Toimil, N.C., 2006. The problem of area change in tangential longitudinal strain folding. Journal of Structural Geology 28, 1835–1848.

Bobillo-Ares, N.C., Bastida, F., Aller, J., 2000. On tangential longitudinal strain folding. Tectonophysics 319, 53–68.

Bobillo-Ares, N.C., Toimil, N.C., Aller, J., Bastida, F., 2004. 'FoldModeler': a tool for the geometrical and kinematic analysis of folds. Computers & Geosciences 30, 147–159.

Cosgrove, J.W., 1980. The tectonic implications of small scale structures in the Mona Complex of Holy Isle, North Wales. Journal of Structural Geology 2, 383–396.

Coward, M.P., 1973. The structure and origin of areas anomalously of low-intensity finite deformation in the basement gneiss complex of the Outer Hebrides. Tectonophysics, 117–140.

Fernández, F.J., Aller, J., Bastida, F., 2007. Kinematics of a kilometric recumbent fold: the Courel syncline (Iberian massif, NW Spain). Journal of Structural Geology 29, 1650–1664.
González-Bonorino, F., 1960. The mechanical factor in the formation of schistosity. In: 21st International Geological Congress, Copenhagen, Pt. 18, pp. 303–316.
Hudleston, P.J., 1973. The analysis and interpretation of minor folds developed in the Moine rocks of Monar, Scotland. Tectonophysics 17, 89–132.
Hudleston, P.J., 1977. Similar folds, recumbent folds, and gravity tectonics in ice and rocks. Journal of Geology 85, 113–122.
Lisle, R.J., 1988. Anomalous vergence patterns on the Rhoscolyn Anticline, Anglesey: implications for structural analysis of refolded regions. Geological Journal 23, 211–220.
Mukhopadhyay, D., 1965. Effects of compression on concentric folds and mechanism of similar folding. Journal of the Geological Society of India 6, 27–41.
Ragan, D.M., 1968. Structural Geology. An Introduction to Geometrical Techniques. John Wiley & Sons, New York.
Ramberg, H., 1963. Strain distribution and geometry of folds. Bulletin of the Geological Institution of the University of Upsala 42, 1–20.
Ramsay, J.G., 1961. The effects of folding on the orientation of sedimentation structures. Journal of Geology 69, 84–100.
Ramsay, J.G., 1962. The geometry and mechanics of formation of "similar" type folds. Journal of Geology 70, 309–327.
Ramsay, J.G., 1963. The folding of angular unconformable sequences. Journal of Geology 71, 297–400.
Ramsay, J.G., 1967. Folding and Fracturing of Rocks. Mc-Graw Hill Book Company, New York.
Ramsay, J.G., Huber, M.I., 1987. Modern Structural Geology. In: Folds and Fractures, vol. 2. Academic Press, London.
Ramsay, J.G., Lisle, R.J., 2000. Modern Structural Geology. In: Applications of Continuum Mechanics in Structural Geology, vol. 3. Academic Press, London.
Ramsay, J.G., Casey, M., Kligfield, R., 1983. Role of shear in development of the Helvetic fold-thrust belt of Switzerland. Geology 11, 439–442.
Toimil, N.C., Fernández, F.J., 2007. Kinematic analysis of symmetrical natural folds developed in competent layers. Journal of Structural Geology 29, 467–480.
Treagus, S.H., Treagus, J.E., Droop, G.T.R., 2002. Superposed deformations and their hybrid effects: the Rhoscolyn Anticline unravelled. Journal of the Geological Society, London 159, 117–136.
Whitten, E.H.T., 1966. Structural Geology of Folded Rocks. Rand McNally & Company, Chicago.
Williams, P.F., 1979. The development of asymmetrical folds in a cross-laminated siltstone. Journal of Structural Geology 1, 19–30.